

Dilatonic (Anti-)de Sitter Black Holes and Weak Gravity Conjecture

Karim Benakli^{a,*}

^a*Laboratoire de Physique Théorique et Hautes Energies (LPTHE), UMR 7589, Sorbonne Université et CNRS,*

4 place Jussieu, 75252 Paris Cedex 05, France.

E-mail: kbenakli@lpthe.jussieu.fr

We summarize our results on the presence and location of horizons in charged black hole solutions of Einstein-Maxwell-dilaton theory with non-trivial dilaton potentials, asymptotically flat or (Anti-)de Sitter, as function of the black hole parameters mass, charge and dilaton coupling strength. We observe that there is a value of latter which separates two regions, one where the black hole is Reissner-Nordström-like from a region where it is Schwarzschild-like. We find that for de Sitter and small non-vanishing of the dilaton coupling parameter, the extremal case is not reached by the solution. We also discuss the attractive or repulsive nature of the leading long distance interaction between two such black holes, or a test particle and one black hole, from a world-line effective field theory point of view.

*Corfu Summer Institute 2021 "School and Workshops on Elementary Particle Physics and Gravity"
29 August - 9 October 2021
Corfu, Greece*

*Speaker

1. Introduction

The Einstein-Maxwell-dilaton action reads

$$\mathcal{S} = \int d^4x \sqrt{-g} \frac{1}{2\kappa^2} \left(R - 2(\partial\phi)^2 - e^{-2\alpha\phi} F^2 - V(\phi) \right), \quad (1)$$

where R is the Ricci scalar, $F_{\mu\nu}$ is the $U(1)$ field strength and Λ the cosmological constant. Denoting $g = e^{\alpha\phi}$ as the gauge couplings $g = e^{\alpha\phi}$, then:

$$V(\phi) = \frac{2}{3} \frac{\Lambda}{(1+\alpha^2)^2} \left[\alpha^2(3\alpha^2-1) \left(\frac{g}{g_0} \right)^{-2/\alpha^2} + (3-\alpha^2) \left(\frac{g}{g_0} \right)^2 + 8\alpha^2 \left(\frac{g}{g_0} \right)^{1-1/\alpha^2} \right], \quad (2)$$

with the asymptotic value $g_0 = e^{\alpha\phi_0}$ with ϕ_0 the asymptotic value of $\phi(r)$ for $r \rightarrow \infty$. For $\alpha = 1$:

$$V(\phi) = \frac{1}{3} \Lambda \left[\frac{g_0^2}{g^2} + \frac{g^2}{g_0^2} + 4 \right]. \quad (3)$$

where one could associate the first, second and third terms to D -brane fluxes, one-loop effect and tree-level cosmological constant contributions, respectively. Further discussion of this potential can be found in [1].

A spherically symmetric solution describing a black hole metric is given by:

$$\left\{ \begin{array}{l} ds^2 = - \left[\left(1 - \frac{r_{\pm}}{r}\right) \left(1 - \frac{r_{\mp}}{r}\right)^{\frac{1-\alpha^2}{1+\alpha^2}} \mp H^2 r^2 \left(1 - \frac{r_{\mp}}{r}\right)^{\frac{2\alpha^2}{1+\alpha^2}} \right] dt^2 \\ \quad + \left[\left(1 - \frac{r_{\pm}}{r}\right) \left(1 - \frac{r_{\mp}}{r}\right)^{\frac{1-\alpha^2}{1+\alpha^2}} \mp H^2 r^2 \left(1 - \frac{r_{\mp}}{r}\right)^{\frac{2\alpha^2}{1+\alpha^2}} \right]^{-1} dr^2 \\ \quad + r^2 \left(1 - \frac{r_{\mp}}{r}\right)^{\frac{2\alpha^2}{1+\alpha^2}} d\Omega_2^2, \\ e^{2\alpha\phi} = e^{2\alpha\phi_0} \left(1 - \frac{r_{\mp}}{r}\right)^{\frac{2\alpha^2}{1+\alpha^2}}, \\ F = \frac{1}{\sqrt{4\pi G}} \frac{Q e^{2\alpha\phi_0}}{r} dt \wedge dr. \end{array} \right. \quad (4)$$

where the parameters M and Q are related to the charge \tilde{Q} and mass \tilde{M} through:

$$M = \frac{\kappa^2 \tilde{M}}{8\pi}, \quad Q^2 = \frac{\kappa^2 \tilde{Q}^2}{32\pi^2} \quad \Rightarrow \quad \frac{M^2}{Q^2} = \frac{\kappa^2 \tilde{M}^2}{2 \tilde{Q}^2}, \quad (5)$$

with $\kappa^2 = 1/M_P^2 = 8\pi G \equiv 8\pi$ and G Newton's constant. H^2 is the Hubble parameter $H^2 = |\Lambda|/3$. The $\Lambda = 0$ corresponds to the asymptotically flat black hole solution [2, 3], upper sign to an asymptotically dS, lower sign to AdS space-time. These solutions have only two independent parameters r_+ , r_- (with an appropriate choice of signs [1])

$$\left\{ \begin{array}{l} r_+ = M + \sqrt{M^2 - (1-\alpha^2)Q^2 e^{2\alpha\phi_0}} \\ r_- = \frac{(1+\alpha^2)Q^2 e^{2\alpha\phi_0}}{M + \sqrt{M^2 - (1-\alpha^2)Q^2 e^{2\alpha\phi_0}}}, \end{array} \right. \quad (6)$$

- When $\alpha \geq 1$: the $r_+ \geq [(\alpha^2 - 1)/(\alpha^2 + 1)] r_-$ part of the (r_+, r_-) plane describes the whole (M, Q) one. The portion $r_+ < [(\alpha^2 - 1)/(\alpha^2 + 1)] r_-$ corresponds to the unphysical negative masses $M < 0$.

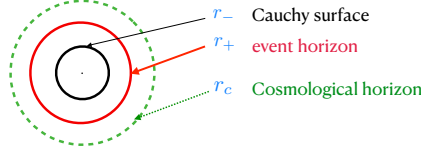


Figure 1: Cauchy and horizon surfaces for de Sitter black holes with a not too large mass and a small enough charge.

- When $0 < \alpha < 1$: $M^2 < (1 - \alpha^2)Q^2 e^{2\alpha\phi_0}$ is not allowed as r_+, r_- and the metric become complex. Therefore, a part of the (M, Q) plane is *inaccessible* to the solution. Again, the region $r_+ < |(1 - \alpha^2)/(1 + \alpha^2)|r_-$ is unphysical.

For Reissner-Nordström solutions with $\alpha = 0$, r_+ and r_- do not appear separately in the metric, but only through the combinations $r_+ + r_-$ and $r_+ r_-$ thus there is no issue of complex valued metrics. When $\alpha \neq 0$, r_- is the location of a singular surface while r_+ is the only event horizon of the black hole. The condition for the singularity to be shielded by the horizon is simply $r_+ > r_-$, that is:

$$Q^2 e^{2\alpha\phi_0} < (1 + \alpha^2) M^2 \quad (7)$$

In this case of asymptotically flat black holes, the complex valued region is beyond the reach of the black hole solution.

2. Dilatonic de Sitter Black Holes: $\Lambda > 0$

2.1 $\alpha = 0$ and $\Lambda > 0$

When $\alpha = 0$, the dilaton decouples and we recover the Reissner-Nordström-de Sitter solution studied in [4].

The horizons of this dS-RN black hole metric are discussed in details in [4, 9]. They are obtained by studying the roots of the quartic polynomial:

$$P(r) \equiv -r^2 f(r) = l^{-2} r^4 - r^2 + 2Mr - Q^2. \quad (8)$$

as function of the parameters M, Q, l . The condition for the existence of the black hole is

$$Q^2 \leq M^2 + M^4 H^2 + O(M^6 H^4) \quad (9)$$

with $M^2 H^2 \leq \frac{2}{27}$. The phase space is illustrated in Figure 2.

2.2 $\alpha = 1$ and $\Lambda > 0$

For $\alpha \neq 0$, one needs to distinguish between several cases, corresponding to different behaviours of g_{00} . Here, r_+ does not determine the location of the horizon anymore, while r_- still indicates the coordinate of a singular surface.

thus $P(R_+) < 0$ when $Q(D) > 0$. If $Q(0) > 0$, $Q(D) > 0$ for all D . If $Q(0) < 0$, then there exist a value $D = D_0$ such that $Q(D_0) = 0$:

$$\left\{ \begin{array}{l} D < D_0 \rightarrow Q(D) < 0 \Rightarrow P(R_+) > 0 \Rightarrow P(r) \neq 0, \forall r \in \mathbb{R}^+ \\ D = D_0 \rightarrow Q(D) = 0 \\ D > D_0 \rightarrow Q(D) > 0 \Rightarrow P(R_+) < 0. \end{array} \right.$$

Imposing the necessary condition $D^2 H^2 < \frac{1}{4}$, we shall now group all cases. There are three possibilities corresponding to 0, 1 or 2 roots.

- P has two roots: $D < M$ and $D > D_1$. Otherwise if $D < M$ and $D < D_1$, then $M^2 H^2 < \frac{1}{27}$ or $M^2 H^2 \geq \frac{1}{27}$ and $Q(D) > 0 \Leftrightarrow D > D_0$.
- P has one root: $D \geq M$ (one of the two roots above is behind the singularity) or $D \leq M$ and $P(R_+) = 0$, $D = D_0$ with $D < D_1$ (the two horizons discussed above coincide).
- P has no root: $D < M$, $D < D_1$, $D < D_0$ and $M^2 H^2 > \frac{1}{27}$.

The results are represented in figure 3:

- The green curve corresponds to $D = D_0$,
- The yellow one to $M = D$. Below, the metric describes a naked singularity with a cosmological horizon.
- In the region between the green and the yellow curves, gives the region where black hole solutions have two horizons. For $Q = 0$, $M = \frac{1}{\sqrt{27}H}$, limits the regions with two and zero horizons.
- The dashed blue curve the function D_1 , is below $M = D$ for $D^2 H^2 < \frac{1}{4}$, is only there for comparison with the flat space-time case.
- The red curve is defined by $2DH = 1$. On its right, the singularity radius is bigger than the Hubble radius.

2.3 $\alpha > \frac{1}{\sqrt{3}}$ and $\Lambda > 0$

The case $\alpha = 1$ could have been solved explicitly. Instead, it was treated with a method that can be generalized to other values of $\alpha \neq 1$ where the equations can not be solved analytically.

First, note that in the $\alpha \rightarrow \infty$ limit of (4), the Schwarzschild-de Sitter solution can be recovered: the sign of $M - \frac{1}{\sqrt{27}H}$ separates between metrics describing naked and shielded singularities.

Second, for generic value of α , we construct a function $F(r) \equiv A(r) + B(r)$ that vanishes for the same values of r than g_{00} and that can be split in two parts that are easy to study graphically:

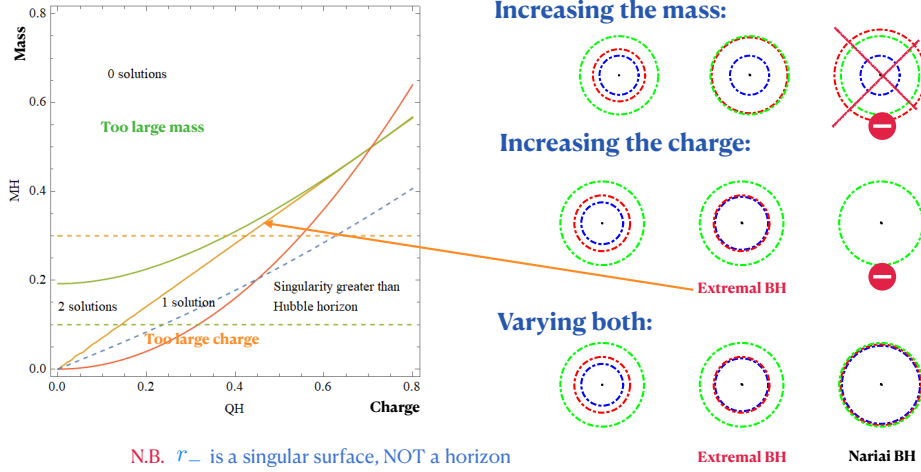


Figure 3: $\alpha = 1$ and $\Lambda > 0$ black holes. Starting with a not too large mass and a small enough charge, one has three horizons (the blue area), then changing the mass and the charge, one can describe the different parts of the diagram. On the right, the relative location of the would-be horizon surfaces are represented. The no-go sign corresponds to naked singularity while in the crossed figure the black hole has "eaten" the de Sitter space patch.

$A(r) \equiv r - r_+$, and $B(r) \equiv H^2 r^3 \left(1 - \frac{r_-}{r}\right)^{\frac{3\alpha^2-1}{\alpha^2+1}}$. The intersection points of the two curves defined by A and B give the zeros of F .

We find that for $\alpha > 1$, the parameter space can be split following the relative values of r_+ and r_- :

- For $r_+ \leq r_-$, $A(r_-) \geq 0$ and $F(r)$ has only one zero, corresponding to the cosmological horizon.
- For $r_+ > r_-$, $A(r_-) < 0$, here can be two, one or zero solutions for $F(r) = 0$.

The detailed analysis is given in [1] where we have chosen for the purpose a value $\alpha = 2$.

2.4 $0 < \alpha < \frac{1}{\sqrt{3}}$ and $\Lambda > 0$

This is probably the case with the newest, unexpected, feature: the extremal case is not reached. To reach the extremal case, for a fixed mass, one needs to increase the black hole charge. But as one tries to go beyond $Q^2 e^{2\alpha\phi_0} = \frac{M^2}{(1-\alpha^2)}$, the metric becomes complex.

Consider two particles, approximative description of two black holes very far away of each other with the same mass ($m(\phi) = M$) and charge ($q = Q$). The overall force is proportional to $M^2 + \alpha MD - e^{2\alpha\phi} Q^2$. The force between these two states can be obtained from the approximate non-relativistic potential $V_{\text{eff}}(r)$:

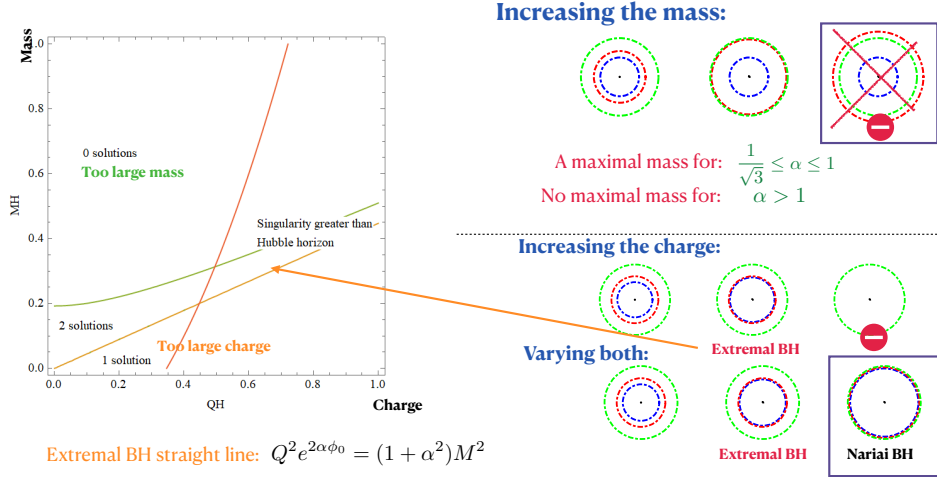


Figure 4: $\alpha > \frac{1}{\sqrt{3}}$ and $\Lambda > 0$ black holes. Starting with a not too large mass and a small enough charge, one has three horizons (the blue area), then changing the mass and the charge, one can describe the different parts of the diagram. On the right, the relative location of the would-be horizon surfaces are represented. The no-go sign corresponds to naked singularity while in the crossed figure the black hole has "eaten" the de Sitter space patch.

$$\begin{aligned}
 V_{\text{eff}}(r) = & -\frac{m_0 M + m'_0 D - e^{2\alpha\phi_0} q Q}{r} \\
 & -\frac{1}{2r^2} \left[\frac{e^{4\alpha\phi_0} q^2}{m_0^2} Q^2 - (1 - \alpha^2) (e^{2\alpha\phi_0} Q^2 - D^2) - \frac{1}{2} \frac{E^2}{m_0^2} D^2 \frac{m''_0{}^2}{m_0^2} \right. \\
 & \left. + \frac{E^2}{m_0^2} \frac{1 + \alpha^2}{\alpha} D^2 \frac{m'_0}{m} - 4 \frac{E}{m_0} e^{2\alpha\phi_0} \frac{q}{m_0} Q D \frac{m'_0}{m_0} + 4 \frac{E^2}{m_0^2} D^2 \left(\frac{m'_0}{m_0} \right)^2 \right] + O\left(\frac{1}{r^3}\right).
 \end{aligned} \tag{14}$$

This force vanishes for $M^2 = \frac{e^{2\alpha\bar{\phi}} Q^2}{1 + \alpha^2}$ and $M^2 = (1 - \alpha^2) e^{2\alpha\bar{\phi}} Q^2$. The latter is the limit where the metric will become complex. Moreover, the amplitude for emission of a pair of dilatons by the point-like particle diverges at this point for $\alpha < 1$.

3. Dilatonic Anti-de Sitter Black Holes

In the AdS case, we study of the zeros of the much simpler function:

$$F_{AdS}(r) \equiv r - r_+ + H^2 r^3 \left(1 - \frac{r_-}{r}\right)^{\frac{3\alpha^2 - 1}{1 + \alpha^2}} = -r \left(1 - \frac{r_-}{r}\right)^{\frac{1 - \alpha^2}{1 + \alpha^2}} g_{00}(r). \tag{15}$$

For $r_+ < r_-$, $F_{AdS} > 0$ for all $r \in [r_-, \infty[$. Again, we split $F_{AdS} = A_{AdS} + B_{AdS}$ with $A_{AdS}(r) \equiv r - r_+$, and $B_{AdS}(r) \equiv -H^2 r^3 \left(1 - \frac{r_-}{r}\right)^{\frac{3\alpha^2 - 1}{1 + \alpha^2}}$ which is always negative. In this way, the problem is again recast in terms of the intersection points of A_{AdS} and B_{AdS} . We split the discussion into three parts depending on the value of α .

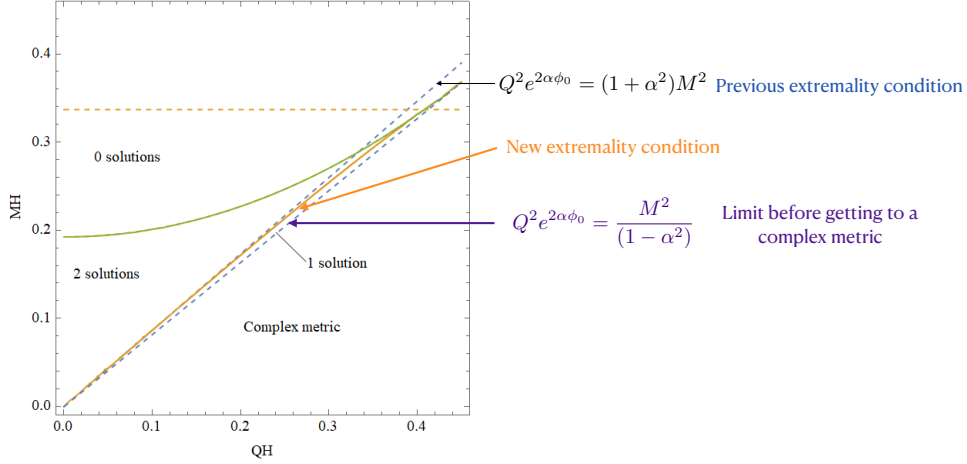


Figure 5: $\alpha = \frac{1}{\sqrt{3}}$ and $\Lambda > 0$ black holes. Starting with a not too large mass and a small enough charge, one has three horizons (the blue area), then changing the mass and the charge, one can describe the different parts of the diagram. On the right, the relative location of the would-be horizon surfaces are represented. The no-go sign corresponds to naked singularity while in the crossed figure the black hole has "eaten" the de Sitter space patch.

$\alpha^2 > \frac{1}{3}$: the discriminant between the black hole regime and the naked singularity is given by $r_+ = r_-$ i.e. $Q^2 e^{2\alpha\phi_0} = (1 + \alpha^2)M^2$.

$\alpha^2 = \frac{1}{3}$: $F_{AdS}(r) = r - r_+ + H^2 r^3$ and the condition of absence of a naked singularity is given in [1].

$\alpha^2 < \frac{1}{3}$: Instead of the complex metric issue, the new feature now is the presence of black holes with two horizons.

The extremality condition can be written now for $H \rightarrow 0$ as

$$Q^2 e^{2\alpha\phi_0} = (1 + \alpha^2)M^2 + \alpha^2(1 + \alpha^2)^{\frac{2}{1-\alpha^2}} c M^{\frac{3-\alpha^2}{1-\alpha^2}} H^{\frac{1+\alpha^2}{1-\alpha^2}} + o(M^{\frac{3-\alpha^2}{1-\alpha^2}} H^{\frac{1+\alpha^2}{1-\alpha^2}}). \quad (16)$$

We see that for $\alpha = 1/\sqrt{3}$, it reduces to

$$Q^2 e^{2\alpha\phi_0} = \frac{4}{3}M^2 - \frac{4^3}{3^4}M^4 H^2 + o(M^4 H^2). \quad (17)$$

It is the same equation as for the dS case, with a difference of sign. For $\alpha \rightarrow 0$, the power of H tends to 1, but the coefficient in front vanishes. This is coherent with [9], since there is no linear term in the expansion for small H .

Acknowledgments

We acknowledge the support of the Agence Nationale de Recherche under grant ANR-15-CE31-0002 "HiggsAutomator".

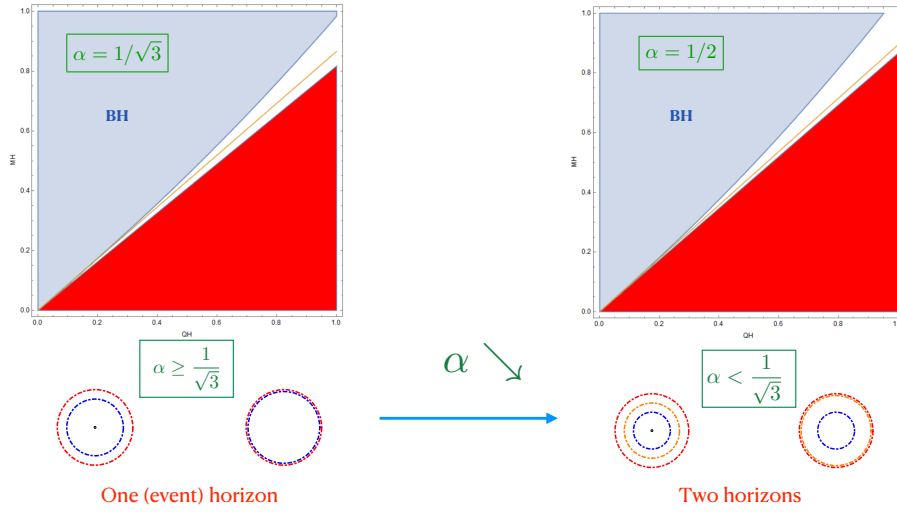


Figure 6: Phase space of black hole in the asymptotically Anti-de Sitter space case.

References

- [1] K. Benakli, C. Branchina and G. Lafforgue-Marmet, *JHEP* **11** (2021), 058 doi:10.1007/JHEP11(2021)058 [arXiv:2105.09800 [hep-th]].
- [2] G. W. Gibbons and K. i. Maeda, *Black Holes and Membranes in Higher Dimensional Theories with Dilaton Fields*, *Nucl. Phys. B* **298** (1988), 741-775
- [3] D. Garfinkle, G. T. Horowitz and A. Strominger, *Charged black holes in string theory*, *Phys. Rev. D* **43** (1991), 3140 [erratum: *Phys. Rev. D* **45** (1992), 3888]
- [4] I. Antoniadis and K. Benakli, *Weak Gravity Conjecture in de Sitter Space-Time*, *Fortsch. Phys.* **68** (2020) no.9, 2000054 [arXiv:2006.12512 [hep-th]].
- [5] K. Benakli, C. Branchina and G. Lafforgue-Marmet, *Revisiting the Scalar Weak Gravity Conjecture*, *Eur. Phys. J. C* **80** (2020) no.8, 742 [arXiv:2004.12476 [hep-th]].
- [6] T. Noumi and J. Tokuda, *Gravitational Positivity Bounds on Scalar Potentials*, [arXiv:2105.01436 [hep-th]].
- [7] F. Kottler, *Über die physikalischen Grundlagen der Einsteinschen Gravitationstheorie*, *Ann. Phys. (Leipzig)* **56** (1918) 410;
D. Kramer, H. Stepani, E. Herlt, M. MacCallum, *Exact solutions of Einstein's field equations* (Cambridge University Press, Cambridge, 1980). 126.
- [8] P. H. Ginsparg and M. J. Perry, *Semiclassical Perdurance of de Sitter Space*, *Nucl. Phys. B* **222** (1983), 245-268.
- [9] L. J. Romans, *Supersymmetric, cold and lukewarm black holes in cosmological Einstein-Maxwell theory*, *Nucl. Phys. B* **383** (1992), 395-415 [arXiv:hep-th/9203018 [hep-th]].

- [10] C. J. Gao and S. N. Zhang, *Dilaton black holes in de Sitter or Anti-de Sitter universe*, Phys. Rev. D **70** (2004), 124019 [arXiv:hep-th/0411104 [hep-th]].
- [11] H. Elvang, D. Z. Freedman and H. Liu, *From fake supergravity to superstars*, JHEP **12** (2007), 023 [arXiv:hep-th/0703201 [hep-th]].
- [12] S. Mignemi, *Exact solutions of dilaton gravity with (anti)-de Sitter asymptotics*, Mod. Phys. Lett. A **29** (2014), 1450010 [arXiv:0907.0422 [gr-qc]].
- [13] K. Goto, H. Marrochio, R. C. Myers, L. Queimada and B. Yoshida, *Holographic Complexity Equals Which Action?*, JHEP **02** (2019), 160 [arXiv:1901.00014 [hep-th]].
- [14] M. Cvetič, G. W. Gibbons and C. N. Pope, *Photon Spheres and Sonic Horizons in Black Holes from Supergravity and Other Theories*, Phys. Rev. D **94** (2016) no.10, 106005 [arXiv:1608.02202 [gr-qc]].
- [15] A. Bedroya and C. Vafa, JHEP **09** (2020), 123 doi:10.1007/JHEP09(2020)123 [arXiv:1909.11063 [hep-th]].
- [16] E. Witten, *Quantum gravity in de Sitter space*, [arXiv:hep-th/0106109 [hep-th]].
- [17] C. F. E. Holzhey and F. Wilczek, *Black holes as elementary particles*, Nucl. Phys. B **380** (1992), 447-477 [arXiv:hep-th/9202014 [hep-th]].
- [18] G. W. Gibbons and S. W. Hawking, *Cosmological Event Horizons, Thermodynamics, and Particle Creation*, Phys. Rev. D **15** (1977), 2738-2751
- [19] F. L. Julié, *Gravitational radiation from compact binary systems in Einstein-Maxwell-dilaton theories*, JCAP **10** (2018), 033 [arXiv:1809.05041 [gr-qc]].
- [20] M. Khalil, N. Sennett, J. Steinhoff, J. Vines and A. Buonanno, *Hairy binary black holes in Einstein-Maxwell-dilaton theory and their effective-one-body description*, Phys. Rev. D **98** (2018) no.10, 104010 [arXiv:1809.03109 [gr-qc]].
- [21] S. Chen and Y. Yang, *Dilaton Mass Formulas in a Hairy Binary Black Hole Model*, Mod. Phys. Lett. A **35** (2020) no.33, 2050277 [arXiv:1904.09944 [gr-qc]].
- [22] T. Shiromizu, *Dilatonic probe, force balance and gyromagnetic ratio*, Phys. Lett. B **460** (1999), 141-147 [arXiv:hep-th/9906177 [hep-th]].
- [23] R. Bousso, *Charged Nariai black holes with a dilaton*, Phys. Rev. D **55** (1997), 3614-3621 [arXiv:gr-qc/9608053 [gr-qc]].